Coupled mode theory analysis of mode-splitting in coupled cavity system

Qiang Li[1], Tao Wang[2], Yikai Su[2], Min Yan[1] and Min Qiu[1]*

[1]*Laboratory of Photonics and Microwave Engineering, School of Information and Communication Technology, Royal Institute of Technology (KTH), Electrum 229, 164 40 Kista, Sweden*

[2]*State Key Laboratory of Advanced Optical Communication Systems and Networks, Department of Electronic Engineering, Shanghai Jiao Tong University, Shanghai 200240, China*

**min@kth.se*

Abstract: We analyze transmission characteristics of two coupled identical cavities, of either standing-wave (SW) or traveling-wave (TW) type, based on temporal coupled mode theory. Mode splitting is observed for both directly (cavity-cavity) and indirectly (cavity-waveguide-cavity) coupled cavity systems. The effects of direct and indirect couplings, if coexisting in one system, can offset each other such that no mode splitting occurs and the original single-cavity resonant frequency is retained. By tuning the configuration of the coupled cavity system, one can obtain different characteristics in transmission spectra, including splitting in transmission, zero transmission, Fano-type transmission, electromagnetically-induced-transparency (EIT)-like transmission, and electromagnetically-induced-absorption (EIA)-like transmission. It is also interesting to notice that a side-coupled SW cavity system performs similarly to an under-coupled TW cavity. The results are useful for the design of cavity-based devices for integration in nanophotonics.

OCIS codes: (350.4238) Nanophotonics and photonic Crystals; (130.3120) Integrated optics devices; (250.5300) Photonic integrated circuits; (230.4555) Coupled resonators

References and links

1. F. Xia, L. Sekaric, and Y. A. Vlasov, "Ultra-compact optical buffers on a silicon chip," Nature Photon. **1**, 65-71 (2007).
2. L. Zhang, M. Song, T. Wu, L. Zou, R. G. Beausoleil, and A. E. Willner, "Embedded ring resonators for microphotonic applications," Opt. Lett. **33**, 1978-1980 (2008).
3. M. Notomi, E. Kuramochi, and T. Tanabe, "Large-scale arrays of ultrahigh-*Q* coupled nanocavities," Nature Photon. **2**, 741-747 (2008).
4. S. Xiao, M. H. Khan, H. Shen, and M. Qi, "A highly compact third-order silicon microring add-drop filter with a very large free spectral range, a flat passband and a low delay dispersion," Opt. Express **15**, 14765-14771 (2007).
5. K. Aoki, D. Guimard, M. Nishioka, M. Nomura, S. Iwamoto, and Y. Arakawa, "Coupling of quantum-dot light emission with a three-dimensional photonic-crystal nanocavity," Nature Photonics **2**, 688-692 (2008).
6. M. Eichenfield, R. Camacho, J. Chan, K. J. Vahala, and O. Painter, "A picogram- and nanometre-scale photonic-crystal optomechanical cavity," Nature **459**, 550-555 (2009).
7. T. Sunner, T. Stichel, S. H. Kwon, T. W. Schlereth, S. Hofling, M. Kamp, and A. Forchel, "Photonic crystal cavity based gas sensor," Appl. Phys. Lett. **92**, 261112 (2008).
8. B. E. Little, S. T. Chu, H. A. Haus, J. Foresi, and J. P. Laine, "Microring resonator channel dropping filters," IEEE J. Lightwave Technol. **15**, 998-1005 (1997).
9. M. Okano, S. Kako, and S. Noda. "Coupling between a point-defect cavity and a line-defect waveguide in three-dimensional photonic crystal," Phys. Rev. B **68**, 235110 (2003).

#123785 - $15.00 USD
Received 4 Feb 2010; accepted 26 Mar 2010; published 6 Apr 2010

10. S. Fan, "Sharp asymmetric line shapes in side-coupled waveguide-cavity systems," Appl. Phys. Lett. **80**, 908-910 (2002).
11. Y. Akahane, T. Asano, B. S. Song, and S. Noda, "Fine-tuned high-*Q* photonic-crystal nanocavity," Opt. Express **13**, 1202-1214 (2005).
12. C. Manolatou, M. J. Khan, S. Fan, P. R. Villeneuve, H. A. Haus, and J. D. Joannopoulos, "Coupling of modes analysis of resonance channel add-drop filters," IEEE J. Quantum Electron. **35**, 1322-1331 (1999).
13. M. A. Popovic, C. Manolatou, and M. Watts, "Coupling-induced resonant frequency shifts in coupled dielectric multi-cavity filters," Opt. Express **14**, 1208-1222 (2006).
14. Y. F. Xiao, X. B. Zou, W. Jiang, Y. L. Chen, and G. C. Guo, "Analog to multiple electromagnetically induced transparency in all-optical drop-filter systems," Phys. Rev. A **75**, 063833 (2007).
15. K. Totsuka, N. Kobayashi, and M. Tomita, "Slow light in coupled-resonator-induced transparency," Phys. Rev. Lett. **98**, 213904 (2007).
16. D. D. Smith, H. Chang, K. A. Fuller, A. T. Rosenberger, and R. W. Boyd, "Coupled-resonator-induced transparency," Phys. Rev. A **69**, 063804 (2004).
17. Z. Zhang, M. Dainese, L. Wosinski, and M. Qiu, "Resonance-splitting and enhanced notch depth in SOI ring resonators with mutual mode coupling," Opt. Express **16**, 4621-4630 (2008).
18. B. E. Little, J. Laine, and S. T. Chu, "Surface-roughness-induced contradirectional coupling in ring and disk resonators," Opt. Lett. **22**, 4-6 (1997).
19. J. D. Joannopoulos, S. G. Johnson, J. N. Winn, and R. D. Meade, Photonic crystals: molding the flow of light (second edition) (Princeton University Press, Princeton, 2008).
20. Q. Li, F. F. Liu, Z. Y. Zhang, M. Qiu, and Y. K. Su, "System performances of on-chip silicon microring delay line for RZ, CSRZ, RZ-DB and RZ-AMI signals," J. Lightwave Technol. **26**, 3744-3751 (2008).
21. Y. Li and M. Xiao, "Observation of of quantum interference between dressed states in electromagnetically induced transparency," Phys. Rev. A **51**, 4959-4962 (1995).
22. M. Lezama, S. Barreiro, and A. M. Akulshin, "Electromagnetically induced absorption," Phys. Rev. A **59**, 4732 (1999).
23. X. Yang, M. Yu, D. L. Kwong, and C. W. Wong, "All-optical analog to electromagnetically induced transparency in multiple coupled photonic crystal cavities," Phys. Rev. Lett. **102**, 173902 (2009).
24. Q. Xu, S. Sandhu, M. L. Povinelli, J. Shakya, S. Fan, and M. Lipson, "Experimental realization of an on-chip all-optical analogue to electromagnetically induced transparency," Phys. Rev. Lett. **96**, 123901 (2006).
25. S. Manipatruni, P. Dong, Q. Xu, and M. Lipson, "Tunable superluminal propagation on a silicon micro-chip," Opt. Lett. **33**, 2928-2930 (2008).

1. Introduction

The optical cavity has been a subject of great interest as it is a vital functional building block for filtering, modulating, buffering, and switching for integrated optical processing in nanophotonics [1-4]. Optical cavities can also be applied in the field of quantum information processing [5], optomechanics [6], sensing [7], etc. Generally speaking, optical cavities can be categorized into two groups: standing-wave (SW) cavities and traveling-wave (TW) cavities. Both types of cavities have been researched extensively. The photonic crystal cavity, distributed feed-back cavity are considered as SW cavities while the ring cavity is a typical example of a TW cavity. Interaction between a single optical cavity and a waveguide has been theoretically studied based on the temporal coupled mode theory (CMT) in Refs.[8-12]. When two or more coupled identical cavity modes exist in a system, mode splitting will naturally occur. Previous study on mode splitting in such systems was however restricted to the directly (cavity-cavity) coupled TW cavity mode for add-drop filter application [13]. SW cavity systems or systems with other types of inter-cavity coupling mechanisms are not studied. In this paper, we systematically analyze mode splittings and transmission characteristics for both directly and indirectly (cavity-waveguide-cavity) coupled cavity systems. The cavities are of either SW or TW type. Altogether we treat coupled SW cavity systems with up to ten different configurations as well as coupled TW cavities with six different configurations using CMT. The transmission amplitude, phase and corresponding group delay are considered in all the configurations. It will be shown that both direct and indirect coupling can lead to mode-splitting, and a coupled SW cavity system and a coupled TW cavity system can have the same characteristics in some cases. A coupling quality factor Q_c is introduced to characterize the direct coupling between two cav-

#123785 - $15.00 USD Received 4 Feb 2010; accepted 26 Mar 2010; published 6 Apr 2010

ity modes, which is more convenient to analyze the behavior of cavity system compared with the conventional matrix approach. The coupling between two cavity modes through waveguide is treated as indirect coupling. The mode-splitting resulted from the coupling between cavity modes can lead to different transmission spectra, including splitting in the transmission, zero transmission, Fano-transmission, electromagnetically-induced-transmission (EIT)-like transmission [14-16] and electromagnetically-induced-absorption (EIA)-like transmission. The mode splitting can also affect the phase characteristics of the transmission and lead to different dispersion features. Among our findings, it is interesting to notice that a side-coupled SW cavity system can perform the same functions as an under-coupled TW cavity system.

It is meaningful to point out that mode splitting can also occur in a single TW-cavity system by introducing structural perturbations on the cavity [17, 18]. This is however not within the scope of our study.

This paper is organized as follows. Section 2 gives a detailed analysis of a single SW and TW cavities, which forms the basis for our later discussions. Section 3 analyzes the mode-splitting characteristics of two directly coupled cavity modes. Both symmetrical and asymmetrical waveguide coupling configurations are considered in this section. Section 4 analyzes the mode-splitting characteristics of two indirectly coupled cavity modes. Section 5 presents our findings on two cavity mode with both direct and indirect coupling. Conclusion is given in Section 6.

2. Single SW and TW cavities

In CMT, an overall system is described in terms of a set of weakly coupled components, each of which can be analyzed using general principles [19]. A cavity, for example, is treated as an oscillator in time. For a SW cavity coupled to a waveguide, its cavity mode decays equally into the forward and backward propagating waveguide mode; while for a TW cavity, the cavity mode decays in only one direction due to momentum matching. For characterizing a cavity, we define the following parameters : ω_0 (λ_0) is the resonant frequency (wavelength); a is the cavity mode amplitude; $s_i/s_t/s_r/s_d$ are the incident/transmitted/reflected/dropped waveguide mode amplitudes, which are normalized such that their squared values correspond to incident/transmitted/reflected/dropped power; $1/\tau_i$ and $1/\tau_w$ are decay rates due to intrinsic loss and waveguide coupling loss, respectively; Q_i and Q_w are cavity quality factors related to intrinsic loss and waveguide coupling loss, respectively; Q_t is total quality factor ($1/Q_t = 1/Q_i + 1/Q_w$). Note that in this paper, Q_w denotes the cavity-waveguide coupling and is referred to as "waveguide coupling quality factor", whereas Q_c represents the cavity-cavity and is referred to as "cavity coupling quality factor". The decay rates are related to the cavity quality factors by $Q_i = \omega_0\tau_i/2$ and $Q_w = \omega_0\tau_w/2$. We use δ to normalize the frequency ω, which is defined by $\delta = (\omega - \omega_0)/\omega_0$, and $t(= s_t/s_i)$, $r(= s_r/s_i)$, $d(= s_d/s_i)$ to denote transfer functions for transmitted port, reflected port and dropped port, respectively.

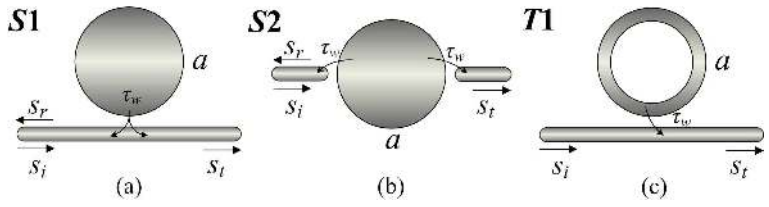

Fig. 1. Schematics of single cavities. (a) and (b) are SW cavities with side-coupling and shoulder-coupling configuration denoted as $S1$ and $S2$, respectively. (c) is a TW cavity denoted as $T1$.

#123785 - $15.00 USD Received 4 Feb 2010; accepted 26 Mar 2010; published 6 Apr 2010

Figure 1 gives the schematics of a single cavity. In this paper, we use a disk and a ring to denote a SW and a TW cavity, respectively. For SW cavities, two different waveguide coupling configurations are considered, including the side-coupling configuration (Fig. 1(a)) and the shoulder-coupling configuration (Fig. 1(b)). Since Q_w denotes the total waveguide coupling quality factor for the mode considered in this paper, it is related to τ_w by $Q_w = \omega_0 \tau_w$ for the $S2$ configuration in Fig. 1(b)(and also for $S4$, $S7$, $S9$, $T4$ and $T6$ in the following discussions). Without loss of generality, we assume the cavity mode is symmetric about the vertical mirror plane perpendicular to the waveguide for $S1$. For the other systems mentioned in this paper, similar assumptions are made to ensure that all waveguide coupling coefficients are the same. According to CMT [11, 12, 20], the transfer functions at the transmitted ports of $S1$, $S2$ and $T1$, denoted by t_{S1}, t_{S2} and t_{T1}, are given in Table 1. For other ports, we can use the relations $r_{S1} = -t_{S2}$ and $r_{S2} = -t_{S1}$. Therefore the transfer functions for the transmitted ports of $S1$ and $S2$ are identical to those for the reflected ports of $S2$ and $S1$, respectively, except with a π phase shift. The transmission T, effective phase shift θ and group delay τ can be calculated as $T = abs(t)^2$, $\theta = \arg(t)$ and $\tau = d\theta(\omega)/d\omega$, respectively; their values at resonance are also given in Table 1.

Table 1. Comparisons between single SW and TW cavities.

	$S1$	$S2$	over-coupled-$T1$	under-coupled-$T1$
t	$\frac{j2\delta+1/Q_i}{j2\delta+1/Q_i+1/Q_w}$	$\frac{1/Q_w}{j2\delta+1/Q_i+1/Q_w}$	$\frac{j2\delta+1/Q_i-1/Q_w}{j2\delta+1/Q_i+1/Q_w}$	
$T(\omega_0)$	$\left(\frac{1}{1+Q_i/Q_w}\right)^2$	$\left(\frac{1}{1+Q_w/Q_i}\right)^2$	$Q_t^2\left(\frac{1}{Q_i}-\frac{1}{Q_w}\right)^2$	
θ	$[-\theta_1,\theta_1] \subset [-\frac{\pi}{2},\frac{\pi}{2}]$	$[-\frac{\pi}{2},\frac{\pi}{2}]$	$[0,2\pi]$	$[-\theta_2,\theta_2] \subset [-\frac{\pi}{2},\frac{\pi}{2}]$
$\theta(\omega_0)$	0	0	π	0
$\tau(\omega_0)$	$-\frac{2Q_i}{Q_w}\frac{Q_t}{\omega_0}$	$\frac{2Q_t}{\omega_0}$	$\frac{4/Q_w}{1/Q_w-1/Q_i}\frac{Q_t}{\omega_0}$	$-\frac{4/Q_w}{1/Q_i-1/Q_w}\frac{Q_t}{\omega_0}$

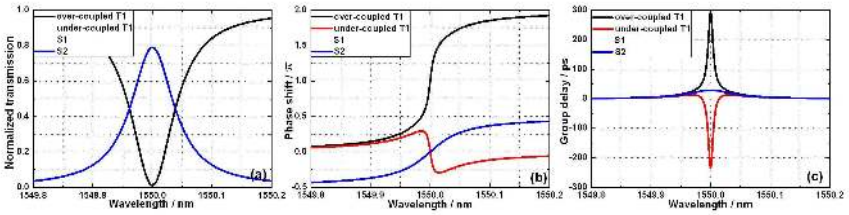

Fig. 2. Transmission, phase shift and group delay of single SW and TW cavity. For $S1$ and $S2$, Q_i=16×10^4, Q_w=2×10^4. For over-coupled $T1$, Q_i=4×10^4, Q_w=3.2×10^4. For under-coupled $T1$, Q_w=4×10^4, Q_i=3.2×10^4. We assume λ_0=1550 nm here and in the following figures.

From the Table 1 and Fig. 2, we can draw the following conclusions:

1. When $Q_{i-over-T1} = Q_{w-under-T1} = 2Q_{w-S1}$ and $1/Q_{w-over-T1} = 1/Q_{i-under-T2} = 1/Q_{i-S1} + 1/(2Q_{w-S1})$, the over-coupled $T1$ (the TW cavity with $Q_i > Q_w$), under-coupled $T1$ (the TW cavity with $Q_i < Q_w$) and $S1$ have identical transmission spectra, as is shown in Fig. 2(a). Especially, the phase shift and group delay are completely the same for under-coupled $T1$ and $S1$. Therefore, we can treat the under-coupled TW cavity as a side-coupled SW cavity. In the following analyses, a system based on under-coupled TW cavities can be replaced with its counterpart based on side-coupled SW cavities.

#123785 - $15.00 USD Received 4 Feb 2010; accepted 26 Mar 2010; published 6 Apr 2010

2. For the SW cavity, the transmission approaches zero for $S1$ and unity for $S2$ when $Q_i \gg Q_w$. For the TW cavity, the transmissivity is unity when $Q_i \gg Q_w$ and zero when $Q_i = Q_w$, i.e, the critical coupling condition satisfied.

3. The over-coupled $T1$ exhibits the largest phase shift range ($\sim 2\pi$). For $S2$, the phase shift range is only π. For $S1$ and under-coupled $T1$, the phase shift ranges are $2\theta_1$ and $2\theta_2$, respectively, where $\theta_1 = tan^{-1}\left[\sqrt{Q_i Q_t}/(2Q_w)\right]$ and $\theta_2 = tan^{-1}\left(1\Big/\sqrt{Q_w^2/Q_i^2 - 1}\right)$. The phase shift range can achieve π only when $Q_i \gg Q_w$ for $S1$ and Q_w approaches Q_i for under-coupled $T1$.

4. The dispersions at resonance for $S2$ and over-coupled $T1$ are normal and thus slow-light can be obtained. While for S1 and under-coupled $T1$, abnormal dispersion occurs at resonance and thus fast-light takes place.

3. Two directly coupled cavity modes

In this section, we analyze the mode-splitting characteristics of two identical cavity modes with direct coupling. Two situations are considered, where the coupling waveguide(s) is(are) placed either symmetrically or asymmetrically. The coupling coefficient between the two cavity modes is denoted by μ and is related to coupling quality factor by $Q_c = \omega_0/(2\mu)$.

3.1. Two directly coupled cavity modes with symmetric coupling waveguides

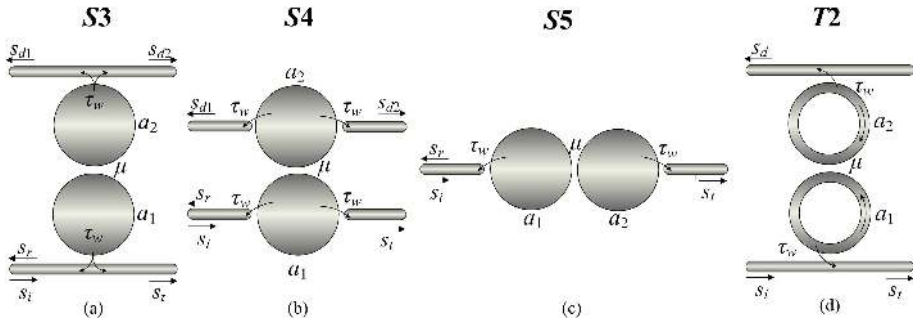

Fig. 3. Schematics of two identical coupled cavity modes with symmetric waveguide coupling. (a)-(c) consist of two SW cavities but with different waveguide coupling configurations ($S3$-$S5$). (d) consists of two TW cavities ($T2$).

Figure 3 shows two identical cavity modes with direct coupling. The coupling waveguides are in symmetric placement. In these cases, the degeneracy of the two cavity modes are lifted due to the coupling, hence a split in the resonant frequencies. For two degenerate SW modes shown in Fig. 3(a), the evolution of fields a_1 and a_2 can be described from the CMT

$$\frac{d}{dt}a_1 = \left(j\omega_0 - \frac{1}{\tau_i} - \frac{1}{\tau_w}\right)a_1 + \sqrt{\frac{1}{\tau_w}}s_i - j\mu a_2 \tag{1}$$

$$\frac{d}{dt}a_2 = \left(j\omega_0 - \frac{1}{\tau_i} - \frac{1}{\tau_w}\right)a_2 - j\mu a_1 \tag{2}$$

Therefore, the transfer functions can be given as

$$t_{S3} = 1 - \frac{1}{2Q_w}\left(\frac{1}{j(2\delta + 1/Q_c) + 1/Q_i + 1/Q_w} + \frac{1}{j(2\delta - 1/Q_c) + 1/Q_i + 1/Q_w}\right) \tag{3}$$

#123785 - $15.00 USD Received 4 Feb 2010; accepted 26 Mar 2010; published 6 Apr 2010

Following the same procedure, the transfer functions for the transmitted ports of $S4$, $S5$ and $T2$ can be given as

$$t_{S4} = \frac{1}{2Q_w}\left(\frac{1}{j\left(2\delta + 1/Q_c\right) + 1/Q_i + 1/Q_w} + \frac{1}{j\left(2\delta - 1/Q_c\right) + 1/Q_i + 1/Q_w}\right) \tag{4}$$

$$t_{S5} = \frac{1}{Q_w}\left(\frac{1}{j\left(2\delta + 1/Q_c\right) + 1/Q_i + 1/Q_w} - \frac{1}{j\left(2\delta - 1/Q_c\right) + 1/Q_i + 1/Q_w}\right) \tag{5}$$

$$t_{T2} = 1 - \frac{1}{Q_w}\left(\frac{1}{j\left(2\delta + 1/Q_c\right) + 1/Q_i + 1/Q_w} + \frac{1}{j\left(2\delta - 1/Q_c\right) + 1/Q_i + 1/Q_w}\right) \tag{6}$$

The transfer functions for the other ports can be obtained through the relations $r_{S3} = t_{S4}$, $d1_{S3} = d2_{S3} = d1_{S4} = d2_{S4} = -t_{S5}/2$, $r_{S4} = -t_{S3}$, $r_{S5} = -t_{T2}$ and $d_{T2} = -t_{S5}$. From Eqs.(3)-(6), we can see that the two degenerate modes with frequency ω_0 are split into two resonant frequencies, namely $\omega_0 - \omega_0/(2Q_c)$ and $\omega_0 + \omega_0/(2Q_c)$. The waveguide coupling quality factor for the two split modes still keeps at Q_w. The separation of the two split resonances is solely determined by the coupling factor Q_c for a fixed ω_0. Figures 4 and 5 illustrate the transmission, phase shift and group delay for the transmitted ports of $S3$-$S5$ and $T2$, respectively.

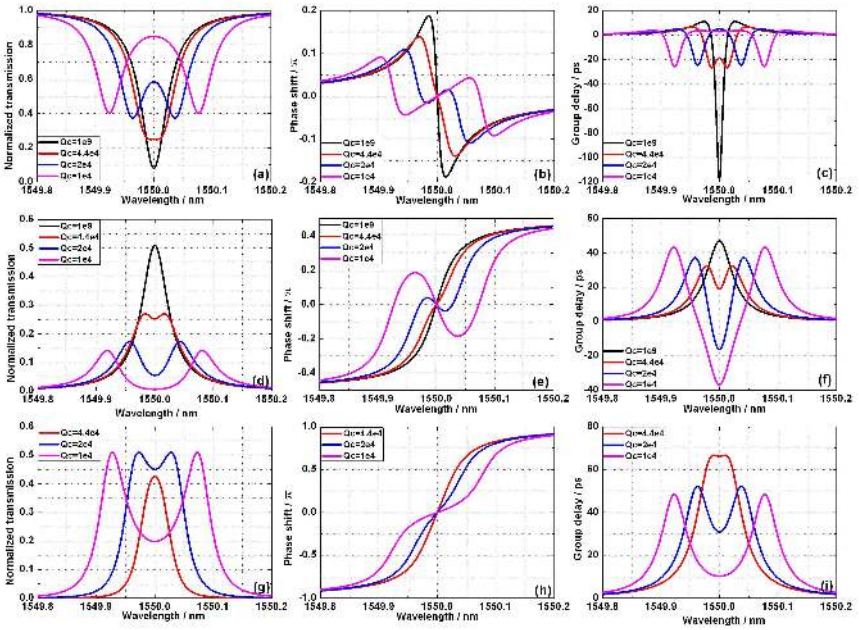

Fig. 4. The transmission, phase shift and group delay for different Q_c for $S3$ (a-c), $S4$ (d-f) and $S5$ (g-i). Q_i=10×10^4, Q_w=4×10^4.

For the SW cavity system $S3$, a decrease in Q_c reduces the depth of resonance notch and further lifts the degeneracy of the two resonances, as shown in Fig. 4(a). The splitting in the transmission turns more and more obvious with increasing coupling. However, the dispersions at the two splittings in the transmission still keep anomalous and thus fast light always takes place, as shown in Fig. 4(b) and (c), respectively. We must point out that although the mode-splitting occurs as long as the coupling exists, it doesn't necessarily mean that the splitting

#123785 - $15.00 USD Received 4 Feb 2010; accepted 26 Mar 2010; published 6 Apr 2010

occurs in the transmission spectrum. This is because that the overall transmission is determined by the superposition of the two split modes with different amplitudes and phases. Here the two splittings can be seen in the transmission only when the coupling is large enough.

For the SW cavity system $S4$, the peak transmission at resonance decreases initially as Q_c decreases. When Q_c decreases further, splitting takes place in the transmission despite that the dispersion remains normal in the two splittings in the transmission, where slow light occurs therefore. The same trends in the transmission, phase shift and group delay occur for the SW cavity system $S5$, which are shown in Fig. 4(g)-(i). The coupling gradually raises the transmission at original resonant wavelength. With decreasing Q_c, splitting manifests itself in the transmission but normal dispersion and slow-light always take place at the two splittings in the transmission.

For the TW cavity system $T2$, we consider two cases: (1) over-coupling case ($Q_i > Q_w$) shown in Fig. 5. As Q_c decreases gradually, the coupling increases resonance notch depth. When $1/Q_c^2 = 1/Q_i^2 - 1/Q_w^2$, the transmission is zero at resonance and there is an abrupt π jump in the phase shift. Once Q_c decreases further, splitting takes place in the transmission and the dispersion at resonances shifts from normal to anomalous. For the dispersion response, slow-light occurs at the enhanced resonance and fast-light at the two splittings in the transmission. (2) under-coupling case ($Q_i < Q_w$). The under-coupled TW cavity can be regarded as a side-coupled SW cavity, as has been pointed out in Section 2. Therefore, the transmission, phase shift and group delay characteristics for $T2$ in this case are completely the same as those for $S3$.

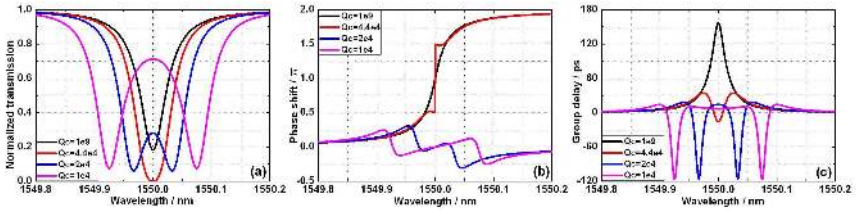

Fig. 5. The transmission, phase shift and group delay for different Q_c for $T2$. Q_i=10×10^4 and Q_w=4×10^4.

#123785 - $15.00 USD Received 4 Feb 2010; accepted 26 Mar 2010; published 6 Apr 2010

3.2. Two directly-coupled cavity modes with asymmetric coupling waveguide(s)

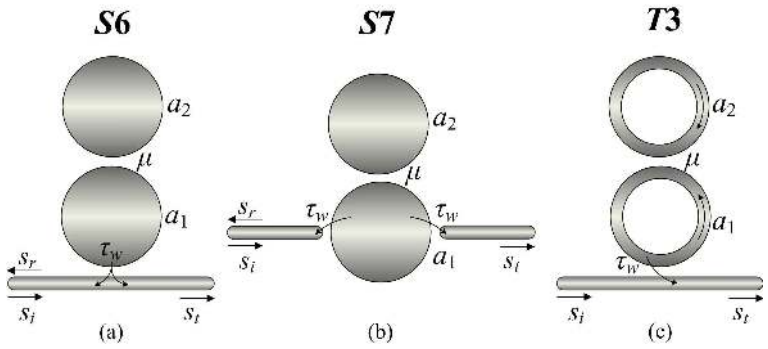

Fig. 6. Schematics of two identical coupled cavity modes with asymmetric waveguide coupling. (a) and (b) consist of two SW cavities with different waveguide-coupling configurations, denoted by $S6$ and $S7$, respectively. (c) consists of two TW cavities denoted by $T3$.

In this part, we analyze the cases that the waveguide-coupling for the two coupled cavity modes are asymmetric, which are shown in Fig. 6. The resonant frequencies for a_1 and a_2 are ω_0 while the intrinsic quality factors are Q_{i1} and Q_{i2}, respectively. The waveguide-coupling occurs only for mode a_1 in all three configurations. For the $S6$ configuration, the CMT equations are given as follows:

$$\frac{d}{dt}a_1 = \left(j\omega_0 - \frac{1}{\tau_{i1}} - \frac{1}{\tau_w}\right)a_1 + \sqrt{\frac{1}{\tau_w}}s_i - j\mu a_2 \tag{7}$$

$$\frac{d}{dt}a_2 = \left(j\omega_0 - \frac{1}{\tau_{i2}}\right)a_2 - j\mu a_1 \tag{8}$$

Therefore, the transfer function can be obtained as follows:

$$t_{S6} = 1 - \frac{1}{Q_w}\frac{j2\delta + \frac{1}{Q_{i2}}}{\left(j2\delta + \frac{1}{2Q_{i2}} + \frac{1}{2Q_{i1}} + \frac{1}{2Q_w}\right)^2 + \left(\frac{1}{Q_c}\right)^2 - \left(\frac{1}{2Q_{i1}} - \frac{1}{2Q_{i2}} + \frac{1}{2Q_w}\right)^2} \tag{9}$$

Following the same procedure, we can obtain the transfer functions for $S7$ and $T3$:

$$t_{S7} = \frac{1}{Q_w}\frac{j2\delta + \frac{1}{Q_{i2}}}{\left(j2\delta + \frac{1}{2Q_{i2}} + \frac{1}{2Q_{i1}} + \frac{1}{2Q_w}\right)^2 + \left(\frac{1}{Q_c}\right)^2 - \left(\frac{1}{2Q_{i1}} - \frac{1}{2Q_{i2}} + \frac{1}{2Q_w}\right)^2} \tag{10}$$

$$t_{T3} = 1 - \frac{2}{Q_w}\frac{j2\delta + \frac{1}{Q_{i2}}}{\left(j2\delta + \frac{1}{2Q_{i2}} + \frac{1}{2Q_{i1}} + \frac{1}{2Q_w}\right)^2 + \left(\frac{1}{Q_c}\right)^2 - \left(\frac{1}{2Q_{i1}} - \frac{1}{2Q_{i2}} + \frac{1}{2Q_w}\right)^2} \tag{11}$$

The transfer functions for other ports can be related to those for the transmitted port: $r_{S6} = -t_{S7}$, $r_{S7} = -t_{S6}$.

#123785 - $15.00 USD Received 4 Feb 2010; accepted 26 Mar 2010; published 6 Apr 2010

Table 2. Mode-splitting characteristic for $S6$ for different coupling strengths.

	resonant frequency	intrinsic quality factor	waveguide coupling quality factor
$\frac{2}{Q_c} > \frac{1}{Q_{i1}} - \frac{1}{Q_{i2}} + \frac{1}{Q_w}$	$\omega_0 - \omega_0/(2Q_0)$ $\omega_0 + \omega_0/(2Q_0)$	$2Q_{i1}Q_{i2}/(Q_{i1}+Q_{i2})$	$2Q_w$
$\frac{2}{Q_c} < \frac{1}{Q_{i1}} - \frac{1}{Q_{i2}} + \frac{1}{Q_w}$	ω_0	$2Q_{i1}Q_{i2}/(Q_{i1}+Q_{i2})$	$2Q_wQ_0/(Q_0+2Q_w)$ $2Q_wQ_0/(Q_0-2Q_w)$
$\frac{2}{Q_c} = \frac{1}{Q_{i1}} - \frac{1}{Q_{i2}} + \frac{1}{Q_w}$	ω_0	$2Q_{i1}Q_{i2}/(Q_{i1}+Q_{i2})$	$2Q_w$

Table 2 provides the mode-splitting characteristic for $S6$ for different coupling strengths. Here $\left(1/Q_0\right)^2 = \left|\left(1/Q_c\right)^2 - \left[1/(2Q_{i1}) - 1/(2Q_{i2}) + 1/(2Q_w)\right]\right|^2$. We can see from Table 2 that the mode-splitting depends greatly on the coupling strength: (1) when $2/Q_c > 1/Q_{i1} - 1/Q_{i2} + 1/Q_w$, the resonant frequency for the two split modes are $\omega_0 - \omega_0/(2Q_0)$ and $\omega_0 + \omega_0/(2Q_0)$, respectively, while the intrinsic quality factor and the waveguide coupling quality factor are the same; (2) when $2/Q_c < 1/Q_{i1} - 1/Q_{i2} + 1/Q_w$, the resonant frequencies for the two split modes are still ω_0 but the waveguide coupling quality factors are different, which are $2Q_wQ_0/(Q_0+2Q_w)$ and $2Q_wQ_0/(Q_0-2Q_w)$, respectively; (3) when $2/Q_c = 1/Q_{i1} - 1/Q_{i2} + 1/Q_w$, the two split modes are degenerate, with the same resonant frequency and intrinsic quality factor and waveguide coupling quality factor. The transmissions for $S6$, $S7$ and $T4$ when $Q_{i2} \to \infty$ are given by the following expressions:

$$T_{S6} = 1 - \frac{\delta^2\left(2/(Q_{i1}Q_w) + 1/Q_w^2\right)}{\delta^2\left(1/Q_{i1} + 1/Q_w\right)^2 + 4\left(\delta^2 - 1/(4Q_c^2)\right)^2} \tag{12}$$

$$T_{S7} = \frac{\delta^2/Q_w^2}{\delta^2\left(1/Q_{i1} + 1/Q_w\right)^2 + 4\left(\delta^2 - 1/(4Q_c^2)\right)^2} \tag{13}$$

$$T_{T3} = 1 - \frac{4\delta^2/(Q_{i1}Q_w)}{\delta^2\left(1/Q_{i1} + 1/Q_w\right)^2 + 4\left(\delta^2 - 1/(4Q_c^2)\right)^2} \tag{14}$$

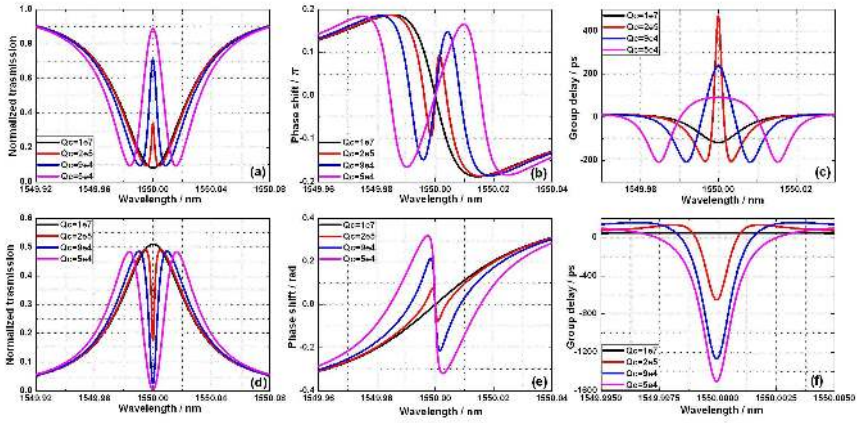

Fig. 7. Illustration of the transmission, phase shift and group delay of cavities for $S6$ (a-c) and $S7$ (d-f). Q_{i1}=10×10^4, Q_w=4×10^4 and Q_{i2}=10×10^5.

#123785 - $15.00 USD
Received 4 Feb 2010; accepted 26 Mar 2010; published 6 Apr 2010

We first recall EIT equation from Ref. [21], $T_{ab} = \Omega_1^2\Gamma\Delta^2 \Big/ \left[\Delta^2\Gamma^2 + 4\left(\Delta^2 - \Omega_2^2/4\right)^2\right]$, where Ω_1 and Ω_2 are respective Rabi frequencies of probe field and pump field, Γ is decay rate and Δ is detuning of probe field from atomic resonance. It can be seen that Eq. 12 is identical to the EIT equation if we regard $\omega_0\delta \to \Delta$, $\omega_0/Q_{i1}+\omega_0/Q_w \to \Gamma$, $\omega_0/Q_c \to \Omega_2$. Therefore, the EIT-like transmission is a special case of mode-splitting due to the coupling between cavity modes. From Eq.12, two conclusions can be drawn: (1) $T(\omega_0) = 1$, meaning that complete transparency can be obtained in the transmission spectrum; (2) T_{S6} achieves minimum at $\delta = 1/(2Q_c)$ and this minimum can be zero if $Q_{i1} \gg Q_w$.

Figure 7 plot the transmission, phase shift and group delay for $S6$ and $S7$. For $S6$, without direct coupling, the dispersion is abnormal and fast-light occurs at resonance. As the direct coupling increases, the EIT-resonance becomes obvious and the dispersion changes to normal in the EIT-like resonance. It can be seen that the delay is quite large at the EIT-like resonance, which is obviously demonstrated in Fig. 7(c) when $Q_c = 2\times10^5$. No complete transparency is achieved because we consider the loss of mode a_2 here.

For $S7$, the transmission at resonance forms a dip with increased direct coupling, which is called EIA. The EIA is an opposite effect of EIT and enhancement of absorption in EIA results from from atomic coherence induced by optical radiation [22]. Here, it originates from the direct coupling between two modes. From Eq.13, we can see that $T(\omega_0) = 0$, meaning that complete absorption occurs in the EIA-like resonance. The dispersion is abnormal and large fast-light occurs in this EIA-like resonance, as are shown in Figs. 7(e) and (f), respectively.

For $T3$, when $Q_c \to \infty$, Eq. 14 is also an EIT equation. Figure 8 provides the transmission, phase shift and group delay for $T3$ when mode a_1 is in over-coupled case ($Q_{i1} > Qc$). As direct coupling increases, a dip appears in the resonance notch first. When $1/Q_c^2 = (1/Q_w - 1/Q_{i1})/Q_{i2}$, $T(\omega_0) = 0$, indicating that zero transmission is achieved with the aid of direct coupling. As the direct coupling increases further, the dip disappears and EIT-like resonance appears. Normal dispersion and large slow-light can be observed in the EIT-like resonance of $T3$, which are the same as that of $S6$. The dispersions are normal in the two splittings, where slow-light occurs. This is different from $S6$, where abnormal dispersion and fast-light occur in the two splittings. For under-coupled case ($Q_{i1} < Q_w$), the transmission, phase shift and group delay are similar to those of $S6$ system.

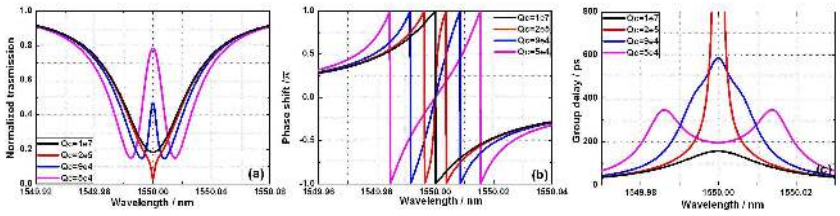

Fig. 8. Illustration of the transmission, phase shift and group delay of cavities for $T3$. Q_{i1}=10×10^4, Q_w=4×10^4 and Q_{i2}=10×10^5.

4. Two indirectly coupled cavity modes

In this part, we analyze two cavity modes coupled through waveguide. For the SW cavity system $S8$ shown in Fig. 9(a), the two cavities are connected by a waveguide, which induces a phase shift of ϕ (we neglect the waveguide dispersion here for simplicity) and thus indirect coupling between the two modes a_1 and a_2. We assume the two modes are degenerate. The resonant frequency, intrinsic quality factor and waveguide coupling quality factor are denoted by ω_0, Q_i and Q_w, respectively. According to the CMT, the equations for the evolution of the cavity

#123785 - $15.00 USD Received 4 Feb 2010; accepted 26 Mar 2010; published 6 Apr 2010

modes a_1 and a_2 in time can be given as follows:

$$\frac{d}{dt}a_1 = \left(j\omega_0 - \frac{1}{\tau_i} - \frac{1}{\tau_w}\right)a_1 + \sqrt{\frac{1}{\tau_w}}s_i + \sqrt{\frac{1}{\tau_w}}\left(-e^{j\phi}\sqrt{\frac{1}{\tau_w}}a_2\right) \tag{15}$$

$$\frac{d}{dt}a_2 = \left(j\omega_0 - \frac{1}{\tau_i} - \frac{1}{\tau_w}\right)a_2 + \sqrt{\frac{1}{\tau_w}}e^{j\phi}\left(s_i - \sqrt{\frac{1}{\tau_w}}a_1\right) \tag{16}$$

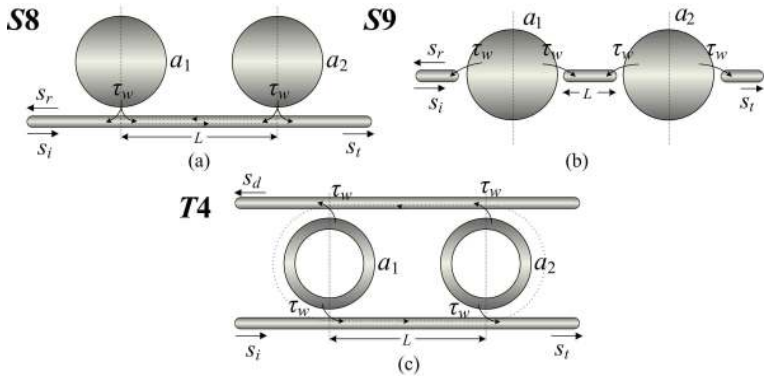

Fig. 9. Schematics of two coupled cavity modes through waveguide. (a) and (b) are two SW cavity modes indirectly coupled through one waveguide ($S8$ and $S9$). (c) is two TW cavity modes indirectly coupled by two waveguides ($T4$).

Therefore, the transfer functions for the transmitted wave and reflected wave can be expressed:

$$t_{S8} = e^{j\phi}\frac{(1-\gamma_0)^2}{1-\gamma_0^2 e^{j2\phi}} \tag{17}$$

$$r_{S8} = \frac{-\gamma_0 - \gamma_0 e^{j2\phi} + 2\gamma_0^2 e^{j2\phi}}{1-\gamma_0^2 e^{j2\phi}} \tag{18}$$

where $\gamma_0 = -1/\left[2Q_w\left(j\delta + 1/(2Q_i) + 1/(2Q_w)\right)\right]$. γ is actually the transfer function of the reflected port for the single side-coupled SW cavity, as has been pointed before. Therefore, the two cavities can be regarded as two reflecting mirrors of a Fabry-Perot etalon. The two mirrors have an amplitude reflectance of γ and transmission of $1+\gamma$. Eqs.(17) and (18) can be regarded as transfer functions for the transmission and reflectance of the Fabry-Perot etalon, respectively. From Eq.(17) for $S8$, we can see that the resonant frequency is modified due to introduction of the waveguide. Eq.(17) can be rewritten as:

$$t_{S8} = e^{j\phi}\left(1 - \frac{\frac{1}{Q_w}\frac{\left(1+e^{j\phi}\right)^2}{2e^{j\phi}}}{j\left(2\delta + \frac{\sin\phi}{Q_w}\right) + \frac{1}{Q_i} + \frac{1+\cos\phi}{Q_w}} + \frac{\frac{1}{Q_w}\frac{\left(1-e^{j\phi}\right)^2}{2e^{j\phi}}}{j\left(2\delta - \frac{\sin\phi}{Q_w}\right) + \frac{1}{Q_i} + \frac{1-\cos\phi}{Q_w}}\right) \tag{19}$$

Table 3 provides the mode-splitting characteristics for $S8$ for different ϕ introduced by the waveguide. We consider three cases here: (1) when ϕ=$m\pi$ (m is an integer), $t_{S8} = (-1)^m\left(j2\delta + 1/Q_i\right)/\left(j2\delta + 1/Q_i + 2/Q_w\right)$, which is the expression for $S1$, except that Q_w is modified to $Q_w/2$. In this case, the two modes a_1 and a_2 can be regarded as one mode with a waveguide coupling quality factor of $Q_w/2$; (2) when ϕ=$(m+1/2)\pi$, the indirect coupling

#123785 - $15.00 USD Received 4 Feb 2010; accepted 26 Mar 2010; published 6 Apr 2010

due to the waveguide leads to mode splitting and the frequencies of the two split modes are $\omega_0 \pm \omega_0 \sin\phi/(2Q_w)$. However, the waveguide coupling quality factors for the two modes are still Q_w. Therefore, the transmission spectrum keeps symmetric. Note that the maximum resonant frequency separation between the two split modes is ω_0/Q_w. (3) when $\phi \neq m\pi/2$, the frequencies of the two split modes are $\omega_0 \pm \omega_0 \sin\phi/(2Q_w)$. Not only the resonant frequency is modified, but also the waveguide coupling quality factors (Q_w) are changed, which is different from the mode-splitting in the direct coupling case. For the mode with a frequency of $\omega_0 + \omega_0 \sin\phi/(2Q_w)$, the waveguide coupling quality factor is modified to $Q_w/(1-\cos\phi)$. For the mode with a frequency of $\omega_0 - \omega_0 \sin\phi/(2Q_w)$, the waveguide coupling quality factor is modified to $Q_w/(1+\cos\phi)$. Figure 11 plots the transmission, phase shift and group delay when $\phi = 0.785$ rad. We can see from Fig. 10 that the transmission ia asymmetrical in this case due to different waveguide coupling quality factors and resonant frequencies of the two split modes. This is actually a kind of Fano-transmission which can be potentially used for lowering power threshold in bistable optical devices and for sensing applications [10].

Table 3. Mode-splitting characteristic for *S*8 for different ϕ introduced by waveguide.

	resonant frequency	intrinsic quality factor	waveguide coupling quality factor
ϕ=$m\pi$	ω_0	Q_i	$Q_w/2$
ϕ=$(m+1/2)\pi$	$\omega_0 + \omega_0 \sin\phi/(2Q_w)$	Q_i	Q_w
	$\omega_0 - \omega_0 \sin\phi/(2Q_w)$		
$\phi \neq m\pi/2$	$\omega_0 + \omega_0 \sin\phi/(2Q_w)$	Q_i	$Q_w/(1-\cos\phi)$
	$\omega_0 - \omega_0 \sin\phi/(2Q_w)$		$Q_w/(1+\cos\phi)$

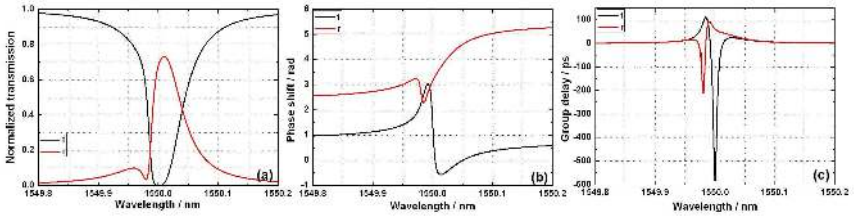

Fig. 10. The transmission, phase shift and group delay for *S*8 system. The black and red lines are for the transmitted port and reflected port, respectively. Q_i=2×10^5 and Q_w=4×10^4. The phase shift induced by the waveguide is ϕ=0.785 rad.

If the two modes are non-degenerate (ω_1 and ω_2), the EIT-like and EIA-like transmission can be obtained, which have been demonstrated in both TW ring cavity and SW PhC cavity [23-25]. Here we just compare this kind of EIT-like transmission with the EIT-like transmission between two degenerate modes shown for the *S*6 system. When $1/\tau_w \gg \omega_1 - \omega_2 \gg 1/\tau_i$ and $\phi = -m\pi$ (m is an integer), the transmission T and reflection $R(= abs(r^2))$ are denoted by $T_{S8} = 1 - \delta^2/Q_w^2 \Big/ \left[\delta^2/Q_w^2 + \left(\delta^2 - \left(\Delta\omega/(2\omega_0)\right)^2\right)^2\right]$ and $R_{S8} = 1 - T_{S8}$, respectively. $\omega_0 = (\omega_1+\omega_2)/2$ and $\Delta\omega = |\omega_1 - \omega_2|$ and $Q_i \to \infty$ is assumed. By comparing with the EIT equation given in Section 3.2, we can see that there are actually the EIT-like resonance and EIA-like resonance for ω_0, if we regard $\omega_0\delta \to \Delta$, $\omega_0/Q_w \to \Gamma$, $\Delta\omega \to \Omega_2$. $T(\omega_0) = 1$ and $T(\omega_1) = T(\omega_2) = 0$. The dashed line in Fig. 9(a) describes the path for EIT-like resonance mode and

#123785 - $15.00 USD Received 4 Feb 2010; accepted 26 Mar 2010; published 6 Apr 2010

thus the phase shift for each round is $2\phi + \arg(\gamma_1) + \arg(\gamma_2)$. The maximum transmission in the EIT-like resonance occurs at $\phi(\omega_0) = -m\pi$. The transmission, phase shift and group delay characteristics are similar to *S*6 system, which are demonstrated in Figs. 7(a)-(c).

For *S*9 system, we can use the CMT to obtain the transfer functions of transmitted port and reflected port. We can also treat the whole system as a Fabry-Perot etalon. The two cavities works as two mirrors. According to the transfer functions for *S*2, the amplitude transmission for the two mirrors are $-\gamma_1$ and $-\gamma_2$ and the amplitude reflectance are $-\gamma_1 - 1$ and $-\gamma_2 - 1$, respectively. Therefore, we can easily obtain the transfer functions for *S*9 system:

$$t_{S9} = \frac{\gamma_1 \gamma_2 e^{j\phi}}{1 - (1+\gamma_1)(1+\gamma_2) e^{j2\phi}} \tag{20}$$

$$r_{S9} = \frac{-(1+\gamma_1) + (1+2\gamma_1)(1+\gamma_2) e^{j\phi}}{1 - (1+\gamma_1)(1+\gamma_2) e^{j2\phi}} \tag{21}$$

Here we just consider the case that the two modes are degenerate ($\gamma_1 = \gamma_2$). Eq. (20) can be rewritten as:

$$t_{S9} = \frac{1/\left(8Q_w^2 \sin\phi\right)}{\left[j\left(\delta + \cot\left(\phi/2\right)/4Q_w\right) + 1/(2Q_i) + 1/(4Q_w)\right]\left[j\left(\delta - \tan\left(\phi/2\right)/4Q_w\right) + 1/(2Q_i) + 1/(4Q_w)\right]} \tag{22}$$

It can be seen from Eq. (22) that the two degenerate resonances are split into two: $\omega_0 - \omega_0 \cot\left(\phi/2\right)/4Q_w$ and $\omega_0 + \omega_0 \tan\left(\phi/2\right)/4Q_w$. The intrinsic quality factor and waveguide coupling quality factor of the two modes are Q_i and $2Q_w$, respectively. Therefore, the resonant frequency separation is quite sensitive to ϕ and can be changed just by adjusting ϕ. This is a distinct feature for *S*9 compared with *S*8. Figure 11plots the transmission, phase shift and group delay for *S*9 when $\phi = -0.2$ rad and $\phi = 1.57$ rad. We can draw two conclusions from Fig. 11 and Eq. (22):

(1) When $0 < \sin^2\phi < {Q_i}^2/(Q_w + Q_i)^2$, there is a splitting in the transmission and the frequencies of the two splittings in the transmission are $\omega_0 - \omega_0\left(\cos\phi \pm \sqrt{1 - (1 + Q_w/Q_i)^2 \sin^2\phi}\right)\Big/(4Q_w \sin\phi)$. When $Q_i >> Q_w$, the two frequencies are ω_0 and $\omega_0 - \omega_0/(2Q_w \tan\phi)$, respectively, and the peak transmission achieves unity. From Figs. 11(a)-(c), we can see that the dispersion and delay characteristics for each splitting are similar to those of *S*2.

(2) When ${Q_i}^2/(Q_w + Q_i)^2 \leq \sin^2\phi \leq 1$, there is no splitting in the transmission although the mode-splitting still exists. The transmission maximum/minimum occurs at $\omega_0 - \omega_0 \cot\phi/(4Q_w)$. From Figs. 11(d)-(e), it is actually a second-order peak filter for the transmitted port and notch filter for the reflected port.

#123785 - $15.00 USD Received 4 Feb 2010; accepted 26 Mar 2010; published 6 Apr 2010

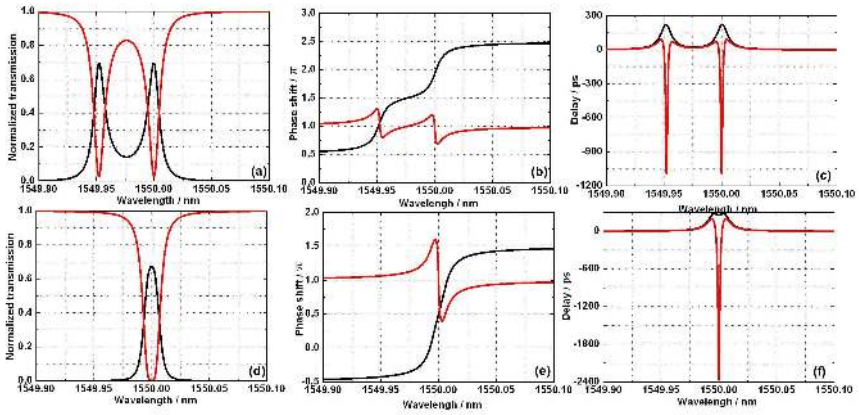

Fig. 11. The transmission, phase shift and group delay for $S9$ system. The black line and red line are for the transmitted port and reflected port, respectively. Q_i=8×10^5 and Q_w=8×10^4. $\phi = -0.2$ rad for (a)-(c) and $\phi = 1.57$ rad for (d)-(f).

For two TW cavity modes indirectly coupled by two waveguides ($T4$) shown in Fig. 9(d), through CMT analysis in [24], its transfer functions are the same as those of two SW cavity modes directly coupled by one waveguide ($S8$), namely $t_{T4} = t_{S8}$ and $d_{T4} = r_{S8}$. Since the resonance mode in $S8$ is standing wave and both forward and backward modes are stimulated simultaneously, the transmission in the waveguide is bi-directional, as is shown in Fig. 9(a); therefore only one waveguide is enough to couple the two standing modes in the two SW cavities. However, for cascaded TW cavity system $T4$, the resonance mode is traveling wave and thus two waveguides are needed to form a closed path for the coupling. The propagation path for the EIT-like resonance mode is shown in Fig. 9(c).

5. Two cavity modes with both indirect and direct couplings

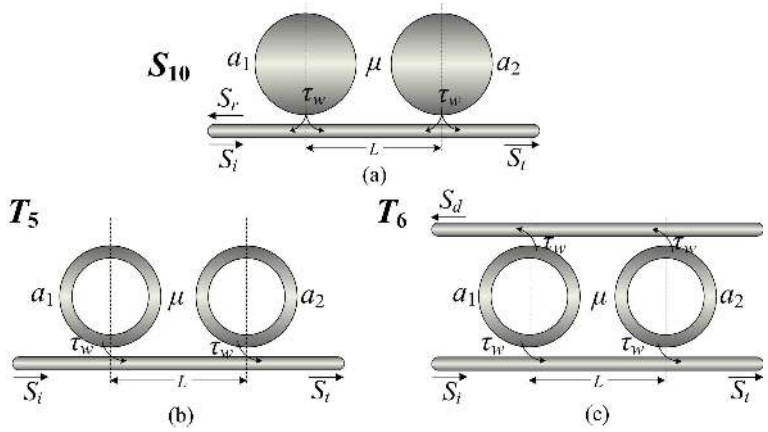

Fig. 12. Schematic of two coupled cavity modes with direct and indirect couplings. (a) two SW cavity modes coupled by one waveguide ($S10$). (b) and (c) are two TW cavity modes coupled by one waveguide ($T5$) and two waveguides ($T6$), respectively.

#123785 - $15.00 USD
Received 4 Feb 2010; accepted 26 Mar 2010; published 6 Apr 2010

In this section, we consider the case that both direct coupling and indirect coupling through waveguide are introduced. The resonant frequencies of the two cavity modes are ω_1 and ω_2, respectively. The quality factors for the two cavity modes are the same. For the system ($S10$) shown in Fig. 12(a), the transfer functions are given by:

$$t_{S10} = e^{j\phi} \frac{1+\gamma_1+\gamma_2+\gamma_1\gamma_2\left(e^{j\phi}+jQ_w/Q_c\right)\left(e^{-j\phi}-jQ_w/Q_c\right)}{1-\gamma_1\gamma_2\left(e^{j\phi}+jQ_w/Q_c\right)^2} \tag{23}$$

$$r_{S10} = \frac{\gamma_1+\gamma_2 e^{j2\phi}+2\gamma_1\gamma_2 e^{j\phi}\left(e^{j\phi}+jQ_w/Q_c\right)}{1-\gamma_1\gamma_2\left(e^{j\phi}+jQ_w/Q_c\right)^2} \tag{24}$$

Here we just consider the case of the two degenerate modes ($\gamma_1 = \gamma_2$). Both direct coupling and indirect coupling through waveguide can lead to mode-splitting and lift the degeneracy of the two resonance modes. For the mode splitting induced by direct coupling, the frequency difference between the two split modes is inversely proportional to the Q_c. For the mode splitting induced by indirect coupling, the frequency difference between the two split modes greatly depends on the phase shift ϕ. From Eq. (23), we can see that these two effects can offset each other so that the original resonant frequency is retained if $\sin\phi = -Q_w/Q_c$. However, we must point out that although the resonant frequencies for these two modes are the same, the waveguide coupling quality factors are modified to $Q_w/(1+2Q_w\cos\phi)$ and $Q_w/(1-2Q_w\cos\phi)$, respectively. Figure 13 provides the transmission, phase shift and group delay for $S10$ system when $\sin\phi = -Q_w/Q_c$ is satisfied. In this case, it turns to be a second order notch filter for the transmission and peak filter for the reflectance.

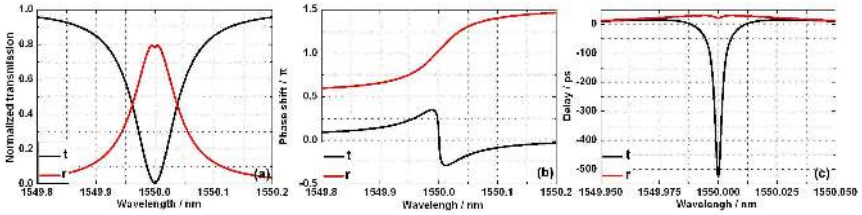

Fig. 13. The transmission, phase shift and group delay of $S10$. The black line (t) and red line (r) denote the transmission for the transmitted port and reflected port, respectively. $Q_w = 4\times10^4$, $Q_i = 2\times10^5$, $Q_c = 4.0067\times10^5$, $\phi = -0.1$ rad.

For two TW cavity modes coupled by one waveguide together with direct coupling ($T5$) shown in Fig. 12(b), we can deduce the transfer function as follows:

$$t_{T5} = e^{j\phi} \frac{1-2\gamma_1-2\gamma_2+\left(4+j2\frac{Q_w}{Q_c}e^{-j\phi}+\frac{Q_w}{Q_c}\frac{Q_w}{Q_c}\right)\gamma_1\gamma_2}{1-j\frac{Q_w}{Q_c}\left(2e^{j\phi}+j\frac{Q_w}{Q_c}\right)\gamma_1\gamma_2} \tag{25}$$

Here we just consider the case that the two modes are degenerate ($\gamma_1 = \gamma_2$). From Eq.(25), we can see that when $Q_w \le 2Q_c$ and $\sin\phi = -1$, the resonant frequencies for the two split modes are still ω_0. The waveguide coupling quality factors are modified to $Q_wQ_c\Big/\left(Q_c+2Q_w\sqrt{Q_w(2Q_c-Q_w)}\right)$ and $Q_wQ_c\Big/\left(Q_c-2Q_w\sqrt{Q_w(2Q_c-Q_w)}\right)$, respectively. Figure 14 provides the transmission, phase shift and group delay for $T5$ system when the mode-splitting due to direct coupling is offset by indirect coupling through waveguide in

#123785 - $15.00 USD Received 4 Feb 2010; accepted 26 Mar 2010; published 6 Apr 2010

resonant frequency. Both the over-coupling ($Q_i > Q_w$) and the under-coupling ($Q_i < Q_w$) cases are provided. In both cases, they are actually second order filter.

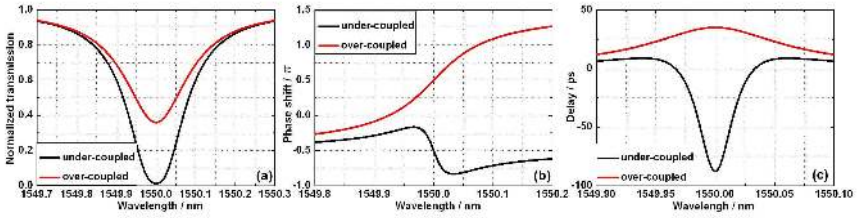

Fig. 14. The transmission, phase shift and group delay of $T5$ when the direct coupling is offset by the indirect coupling through waveguide in resonant frequency. $Q_c = 2 \times 10^4$, $\phi = -1.57$ rad. $Q_w = 4 \times 10^4$ and $Q_i = 2 \times 10^5$ for two under-coupled TW cavities and $Q_w = 2 \times 10^5$ and $Q_i = 4 \times 10^4$ for two over-coupled TW cavities.

For two TW coupled cavity modes with both direct coupling and indirect coupling through two waveguides ($T6$) shown in Fig. 12(d), the transfer functions are completely the same as those of $S10$ system, namely $t_{T6} = t_{S10}$ and $d_{T6} = r_{S10}$.

6. Conclusion

In the paper, the mode-splitting in coupled SW and TW cavities are analyzed based on the temporal CMT. Both the direct coupling and indirect coupling through waveguide can lead to the mode-splitting. For two directly coupled identical cavity modes with symmetrical waveguide coupling configuration ($S3$-$S5$ and $T2$), the resonant frequency is split and the separation between the two resonant frequencies is proportional to the coupling strength. For $T2$ in the over-coupling case, a zero transmission can be obtained by appropriately choosing the coupling. For two directly coupled identical cavity modes with asymmetrical waveguide positioning ($S6$, $S7$ and $T3$), the two split modes can be different either in resonant frequency or in waveguide coupling quality factor, depending on the strength of coupling. In special cases, the EIT-like and EIA-like transmission spectra can be obtained in these configurations. For two coupled cavity modes through indirect waveguide coupling, both the resonant frequency and waveguide coupling quality factor can be different for the two split modes and thus asymmetrical Fano-transmission can be obtained ($S8$ and $T4$). The separation between the two split modes can be easily controlled, in the case for $S9$, by changing the phase shift introduced by the waveguide. The direct and indirect coupling mechanisms can be concurrently deployed in cavity systems to retain original resonant frequency but the waveguide coupling quality factors are still modified ($S10$, $T5$ and $T6$). This research will be useful for the design of cavity-based devices for integration in nanophotonics, either to mitigate the crosstalk due to the coupling between cavities in densely packed photonics chips or to optimize the coupling between cavities for designing new functional photonics devices.

Acknowledgments

This work is supported by the Swedish Foundation for Strategic Research (SSF) and the Swedish Research Council (VR).

#123785 - $15.00 USD Received 4 Feb 2010; accepted 26 Mar 2010; published 6 Apr 2010